

Gregory-Laflamme instability of black hole in Einstein-scalar-Gauss-Bonnet theories

Yun Soo Myung^{a*} and De-Cheng Zou^{a,b†}

^aInstitute of Basic Sciences and Department of Computer Simulation, Inje University
Gimhae 50834, Korea

^bCenter for Gravitation and Cosmology and College of Physical Science and Technology,
Yangzhou University, Yangzhou 225009, China

Abstract

We investigate the stability analysis of Schwarzschild black hole in Einstein-scalar-Gauss-Bonnet (ESGB) theory because the instability of Schwarzschild black hole without scalar hair implies the Gauss-Bonnet black hole with scalar hair. The linearized scalar equation is compared to the Lichnerowicz-Ricci tensor equation in the Einstein-Weyl gravity. It turns out that the instability of Schwarzschild black hole in ESGB theory is interpreted as not the tachyonic instability, but the Gregory-Laflamme instability of black string. In the small mass regime of $1/\lambda < 1.174/r_+$, the Schwarzschild solution becomes unstable and a new branch of solution with scalar hair bifurcates from the Schwarzschild one. This is very similar to finding a newly non-Schwarzschild black hole in Einstein-Weyl gravity.

*e-mail address: ysmjung@inje.ac.kr

†e-mail address: dczou@yzu.edu.cn

1 Introduction

Recently, black hole solutions with scalar hair were found from Einstein-scalar-Gauss-Bonnet (ESGB) theories [1, 2, 3]. These black hole solutions are quite interesting because they show evasion of the novel no-hair theorem [4] which updated the old no-hair theorem [5] by the discovery of black holes with Yang-Mills [6], Skyrme fields [7], or a conformal coupling to gravity [8]. The novel no-hair theorem was extended to cover the standard scalar-tensor theories [9] and a new form covering Galileon fields was proposed [10]. It is worth noting that these with scalar hair are closely related to the instability of black hole without scalar hair. In this theory, the instability of Schwarzschild black hole is determined solely by the linearized scalar equation where the Gauss-Bonnet term acts as an effective mass. This is so because the linearized Einstein equation is nothing but that of the Einstein gravity, where the Regge-Wheeler prescription works to indicate no instability [11, 12].

On the other hand, a fourth-order gravity (Einstein-Weyl gravity) has provided a non-Schwarzschild black hole solution with Ricci tensor hair [13]. Here the Ricci hair means the black hole with non-zero Ricci tensor ($\bar{R}_{\mu\nu} \neq 0$), compared to zero Ricci tensor ($\bar{R}_{\mu\nu} = 0$) for Schwarzschild black hole. Making use of the trace no-hair theorem which states that $\bar{R} = 0$ is zero outside the horizon as well as $\bar{R} \rightarrow 0$ at infinity and on the inner boundary at the horizon [14], they have found the non-Schwarzschild black hole solution which crosses the Schwarzschild solution at the bifurcation point. In this theory, the instability of Schwarzschild black hole was determined by solving the Lichnerowicz equation for the linearized Ricci tensor (so-called Lichnerowicz-Ricci tensor equation) [15, 16, 14]. It has shown that the small black hole in Einstein-Weyl gravity is unstable against $s(l=0)$ -mode of Ricci tensor perturbation, while the large black hole is stable [17]. Actually, this was confirmed by comparing the Lichnerowicz-Ricci tensor equation with the linearized Einstein equation around a five-dimensional black string where the Gregory-Laflamme (GL) instability appeared [18]. In exploring a non-Schwarzschild black hole solution, a static eigenfunction of Lichnerowicz operator has two crucial roles in Einstein-Weyl gravity [19]: a role of perturbation away from Schwarzschild black hole along a non-Schwarzschild black hole and the other role of threshold unstable mode lying at the edge of a domain of GL instability for a small Schwarzschild black hole. We expect that the same thing happens to the black holes found in ESGB theories.

In this work, we will investigate a close connection for instability of black holes found

between ESGB theory and Einstein-Weyl gravity. The linearized scalar equation around Schwarzschild black hole in ESGB theory is surely compared to the Lichnerowicz-Ricci tensor equation around Schwarzschild black hole in the Einstein-Weyl gravity. It turns out that the instability of black hole in ESGB theory is interpreted as the GL instability of black string, even though one uses the linearized scalar equation. In the small mass but not extreme curvature regime, the black hole solution becomes unstable and a new branch of solution with scalar hair bifurcates from the Schwarzschild black hole without scalar hair. This is very similar to finding a non-Schwarzschild black hole with Ricci tensor hair in Einstein-Weyl gravity. Importantly, this will be interpreted as a scalar theory version of the GL instability for a black hole without hair.

2 ESGB theory

Let us start with the ESGB theory [2]

$$S_{\text{ESGB}} = \frac{1}{16\pi} \int d^4x \sqrt{-g} \left[R - 2\partial_\mu \phi \partial^\mu \phi - V_\phi + \lambda^2 f(\phi) \mathcal{R}_{\text{GB}}^2 \right], \quad (1)$$

where ϕ is the scalar field with a potential V_ϕ and a coupling function $f(\phi)$, λ is the GB coupling constant having inverse mass dimension, and $\mathcal{R}_{\text{GB}}^2$ is the GB term defined by

$$\mathcal{R}_{\text{GB}}^2 = R^2 - 4R_{\mu\nu}R^{\mu\nu} + R_{\mu\nu\rho\sigma}R^{\mu\nu\rho\sigma}. \quad (2)$$

In this work, we choose $V_\phi = 0$, but not choose a specific form for $f(\phi)$. Instead, we would like imposing the conditions of $f'(\phi)|_{\phi=0} = 0$ and $f''(\phi)|_{\phi=0} = 1$ and thus, it admits the expansion of $f(\phi) \approx f(0) + \phi^2/2 + \dots$. Examples include $f(\phi) = \frac{1}{2}\phi^2$ [3] and $f(\phi) = \frac{1}{12}[1 - e^{-6\phi^2}]$ [2]. Other examples appeared in Ref. [20]. From the action (1), we derive the Einstein equation

$$G_{\mu\nu} = 2\partial_\mu \phi \partial_\nu \phi - (\partial\phi)^2 g_{\mu\nu} + \Gamma_{\mu\nu}, \quad (3)$$

where $G_{\mu\nu} = R_{\mu\nu} - (R/2)g_{\mu\nu}$ is the Einstein tensor and $\Gamma_{\mu\nu}$ is given by

$$\begin{aligned} \Gamma_{\mu\nu} &= 2R\nabla_{(\mu}\Psi_{\nu)} + 4\nabla^\alpha\Psi_\alpha G_{\mu\nu} - 8R_{(\mu|\alpha|}\nabla^\alpha\Psi_{\nu)} \\ &+ 4R^{\alpha\beta}\nabla_\alpha\Psi_\beta g_{\mu\nu} - 4R^\beta_{\mu\alpha\nu}\nabla^\alpha\Psi_\beta \end{aligned} \quad (4)$$

with

$$\Psi_\mu = \lambda^2 \frac{df(\phi)}{d\phi} \partial_\mu \phi = \lambda^2 f'(\phi) \partial_\mu \phi. \quad (5)$$

On the other hand, the scalar field equation takes the form

$$\square\phi + \frac{\lambda^2}{4} f'(\phi) \mathcal{R}_{\text{GB}}^2 = 0. \quad (6)$$

Choosing $\phi = 0$ and $f'(\phi)|_{\phi=0} = 0$, one finds the Schwarzschild solution from (3) and (6)

$$ds^2 = \bar{g}_{\mu\nu} dx^\mu dx^\nu = -\left(1 - \frac{r_+}{r}\right) dt^2 + \frac{dr^2}{\left(1 - \frac{r_+}{r}\right)} + r^2 d\Omega_2^2 \quad (7)$$

with $r_+ = 2M$. Notice that (7) indicates the black hole solution without scalar hair.

For the stability analysis, we need the two linearized equations which describe the metric perturbation $h_{\mu\nu}$ and scalar perturbation $\delta\phi$ propagating around (7). They are derived by linearizing (3) and (6) as

$$\delta R_{\mu\nu}(h) = 0, \quad (8)$$

$$\left(\bar{\square} + \frac{\lambda^2}{4} \bar{\mathcal{R}}_{\text{GB}}^2\right) \delta\phi = 0. \quad (9)$$

Here the overbar($\bar{\quad}$) denotes computation based on the background spacetime (7). Importantly, we note that “ $-\frac{\lambda^2}{4} \bar{\mathcal{R}}_{\text{GB}}^2$ ” plays a role of not a mass \tilde{m}^2 but an effective mass \tilde{m}_{eff}^2 for $\delta\phi$ because it depends on r . In this sense, the GB coupling term is quite different from a negative mass term like $V_\phi = -m_{\text{T}}^2 \phi^2/2$ with $m_{\text{T}}^2 > 0$ in the tachyonic scalar theory.

For comparison, we would like to mention the Lichnerowicz-Ricci tensor equation around the Schwarzschild black hole in the Einstein-Weyl gravity [15, 17, 16, 14]

$$S_{\text{EW}} = \int d^4x \sqrt{-g} \left[\gamma R - \alpha C_{\mu\nu\rho\sigma} C^{\mu\nu\rho\sigma} \right] \quad (10)$$

where $C_{\mu\nu\rho\sigma}$ is the Weyl tensor. This theory implies the trace no-hair theorem of $R = 0$. Considering the Schwarzschild black hole (7) and linearizing the Einstein equation leads to the Lichnerowicz-Ricci tensor equation for the traceless and transverse Ricci tensor $\delta R_{\mu\nu}$ as

$$\left(\Delta_{\text{L}} + m^2\right) \delta R_{\mu\nu} = 0, \quad m^2 = \frac{\gamma}{2\alpha}, \quad (11)$$

where the Lichnerowicz operator on the Schwarzschild background is given by

$$\Delta_{\text{L}} \delta R_{\mu\nu} = -\bar{\square} \delta R_{\mu\nu} - 2\bar{R}_{\mu\rho\nu\sigma} \delta R^{\rho\sigma}. \quad (12)$$

Here, we emphasize that Eq.(11) is the tensor counterpart to the linearized scalar equation (9). Actually, Eq.(11) describes a massive spin-2 mode ($\delta R_{\mu\nu}$) with mass m propagating on the black hole background. Rewriting Eq.(11) as $(2\alpha\Delta_L + \gamma)\delta R_{\mu\nu} = 0$, one may recover the linearized Einstein equation $\delta R_{\mu\nu} = 0$ in the limit of $\alpha \rightarrow 0$.

3 Instability of black hole without scalar hair

Performing the stability analysis of the black hole, one uses firstly the linearized Einstein equation (8). It turned out that the black hole is stable when making use of the Regge-Wheeler prescription [11, 12]. In this case, a massless spin-2 mode starts with $l = 2$.

Now, let us consider the linearized scalar equation (6). Considering

$$\delta\phi(t, r, \theta, \varphi) = \frac{u(r)}{r} e^{-i\omega t} Y_{lm}(\theta, \varphi), \quad (13)$$

and introducing a tortoise coordinate $r_* = r + r_+ \ln(r/r_+ - 1)$ defined by $dr_* = dr/(1 - r_+/r)$, the radial equation of (9) leads to the Schrödinger-type equation

$$\frac{d^2 u}{dr_*^2} + [\omega^2 - V(r)] u(r) = 0, \quad (14)$$

where the potential $V(r)$ is given by

$$V(r) = \left(1 - \frac{2M}{r}\right) \left[\frac{2M}{r^3} + \frac{l(l+1)}{r^2} - \frac{12\lambda^2 M^2}{r^6}\right]. \quad (15)$$

Moreover, introducing the negative scalar potential $V_\phi = -m_{\text{T}}^2 \phi^2/2$ instead of $-\lambda^2 f(\phi) \mathcal{R}_{\text{GB}}^2$ in Eq.(1), the tachyonic scalar potential takes the form

$$V_{\text{t}}(r) = \left(1 - \frac{2M}{r}\right) \left[\frac{2M}{r^3} + \frac{l(l+1)}{r^2} - m_{\text{T}}^2\right], \quad (16)$$

which induces the tachyonic instability [3] because the sufficient condition for instability ($\int_{2M}^{\infty} dr V_{\text{t}}(r)/(1 - r_+/r) < 0$) is always satisfied with any mass $m_{\text{T}}^2 > 0$. In Minkowski spacetimes, the tachyonic scalar equation takes the form of $\ddot{\varphi}_{\mathbf{k}}(t) + (\mathbf{k}^2 - m_{\text{T}}^2)\varphi_{\mathbf{k}}(t) = 0$, leading to an exponentially growing solution $\varphi_{\mathbf{k}}(t) \sim e^{\sqrt{m_{\text{T}}^2 - \mathbf{k}^2}t}$ for $m_{\text{T}}^2 > \mathbf{k}^2$ [21]. This is an origin of instability arisen from the tachyonic mass.

In the case of $s(l = 0)$ -mode, from the condition of $\int_{2M}^{\infty} dr V(r)/(1 - r_+/r) < 0$, one may introduce a sufficient condition of an unstable bound for a mass parameter of scalar ($1/\lambda$) [2]

$$\frac{M^2}{\lambda^2} < \frac{3}{10} \Rightarrow 0 < \frac{r_+}{\lambda} < 1.095. \quad (17)$$

However, (17) is not a necessary and sufficient condition for instability. Observing Fig. 1 together with $r_+ = 1$, one finds that three potentials $V(r)$ have negative regions near the horizon but they become positive after crossing the r -axis. Surely, these are not types of Regge-Wheeler potentials which are positive definite outside the horizon [11, 12]. It might show a new feature of instability, but the threshold of instability depends on the numerical computations. Importantly, we find a similar behavior from the Zerilli-type potential

$$V_z(r) = \frac{(1 - \frac{1}{r})}{(1 + m^2 r^3)^2} \left[\frac{1}{r^3} - 3m^2(4r - 3) + 3m^4 r^3(2r - 3) + m^6 r^6 \right] \quad (18)$$

for $s(l = 0)$ of Ricci tensor perturbation around the Schwarzschild black hole with $r_+ = 1$ in the Einstein-Weyl gravity (see FIG. 2 in [19]) derived from the linearized equation (11). In addition, we would like to mention that such potentials exist around neutral black holes (black holes without charge) in higher dimensions and the S-deformation used to prove the stability of neutral black holes [22]. This implies that the stability analysis based on the shape of the potential is regarded as a delicate issue. On the other hand, the tachyonic potential $V_t(r)$ indicates a quite different behavior: it develops positive region near the horizon, while it approaches -0.04 as $r \rightarrow \infty$ for $m_T = 0.2$. This shows clearly that the instability of black hole in ESGB theory is not just the tachyonic instability [3] because the sufficient condition for instability ($\int_{2M}^{\infty} dr V_t(r)/(1 - r_+/r) < 0$) is always satisfied with any mass $m_T^2 > 0$.

In order to determine the threshold of instability, one has to solve the second-order differential equation numerically

$$\frac{d^2 u}{dr_*^2} - [\Omega^2 + V(r)] u(r) = 0, \quad (19)$$

which may allow an exponentially growing mode of $e^{\Omega t}$ ($\omega = i\Omega$) as an unstable mode. Here we choose two boundary conditions: a normalizable solution of $u(\infty) \sim e^{-\Omega r_*}$ at infinity and a solution of $u(r_+) \sim (r - r_+)^{\Omega r_+}$ near the horizon. By observing Fig. 2 together with $r_+ = 1, 2, 3$, we read off the unstable bound for scalar mass parameter ($1/\lambda$) as

$$0 < \frac{1}{\lambda} < \left(\frac{1}{\lambda}\right)^{\text{th}} \approx \frac{1.174}{r_+} \quad (20)$$

which implies that the threshold of instability is located at $r_+ = r_c \approx 1.174$ which is greater than 1.095 (sufficient condition for instability). This corresponds to the bifurcation point.

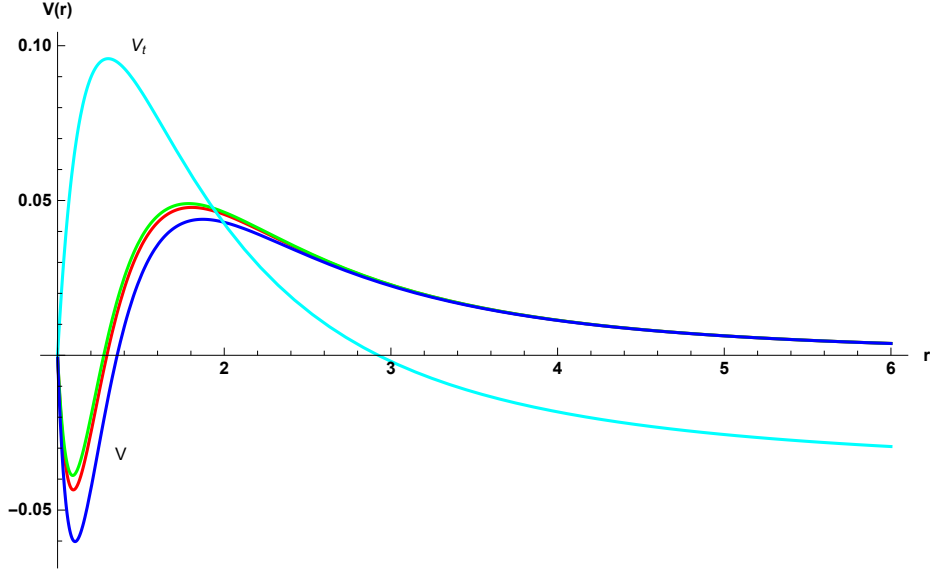


Figure 1: The potentials as function of $r \in [1, \infty)$ for horizon radius $r_+ = 1$ and $l = 0$. The blue (bottom), red (middle), and green (top) curve represent potential $V(r)$ of scalar for mass parameter $1/\lambda = 1.095$ (sufficient condition for instability), 1.174 (threshold of instability), and 1.2 (stable case), respectively. These all have negative regions near the horizon. However, the tachyonic potential (cyan curve) $V_t(r)$ develops positive region near horizon while it approaches -0.04 as $r \rightarrow \infty$ for $m_T = 0.2$.

Choosing $\lambda = 1$, the Schwarzschild black hole will be unstable if its horizon radius satisfies the bound

$$r_+ < r_c \approx 1.174. \quad (21)$$

This implies that the Schwarzschild black hole whose radius is less than the critical radius at the bifurcation point becomes unstable, whereas the black hole whose radius exceeds the critical radius at the bifurcation point is stable.

On the other hand, from Fig. 3 based on Eq.(11), the GL instability mass bound for the $s(l = 0)$ -mode of linearized Ricci tensor δR_{tr} in Einstein-Weyl gravity was given by [17, 14]

$$0 < m < m^{\text{th}} \approx \frac{0.876}{r_+}. \quad (22)$$

Here, selecting $m = 1$, one finds the bound for unstable (small) black holes [19]

$$r_+ < r_c \approx 0.876. \quad (23)$$

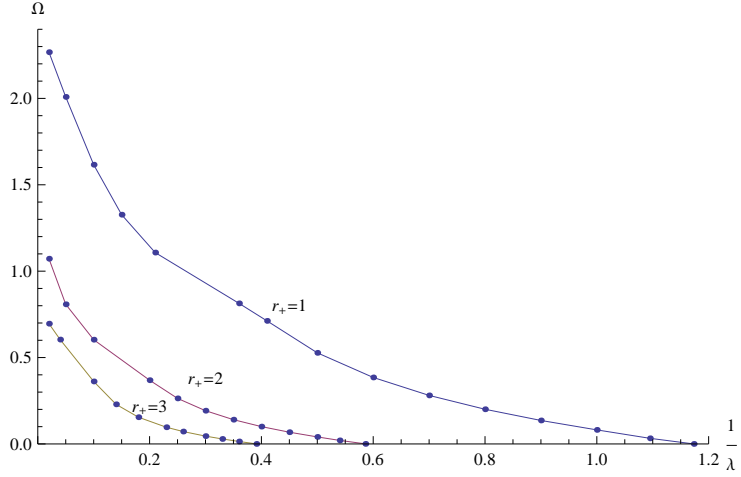


Figure 2: Ω graphs as function of mass parameter $1/\lambda$ for small black holes of $r_+ = 1, 2, 3$. Here, one reads off the thresholds of instability $(1/\lambda)^{\text{th}}$ from the points that curves of Ω intersect the positive $\frac{1}{\lambda}$ -axis: $(1/\lambda)^{\text{th}} \approx 1.174, 0.587, 0.294$. The instability range decreases as the horizon radius increases.

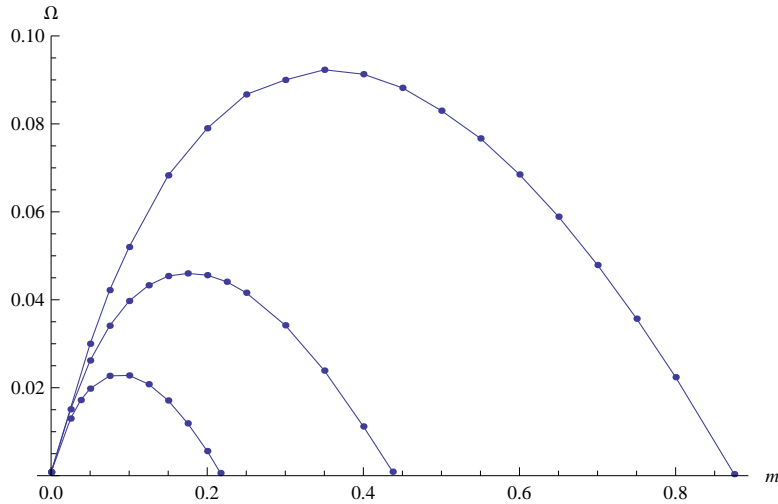


Figure 3: Plots of unstable modes (\bullet) on three curves with the horizon radii $r_+ = 1, 2, 4$. The $y(x)$ -axis denote Ω in $e^{\Omega t}$ (mass m of massive spin-2 mode). The smallest curve represents $r_+ = 4$, the medium denotes $r_+ = 2$, and the largest one shows $r_+ = 1$. Here the thresholds of instability are located at $m^{\text{th}} \approx 0.876, 0.438, 0.219$ which means that the instability region is smaller and smaller as the horizon radius is large and larger.

At this stage, we note that Fig. 2 drawn for s -mode of scalar perturbation is similar to FIG.1 in [23] for s -mode of Ricci tensor perturbation around the non-rotating BTZ black hole in the new massive gravity where the GL instability is reinforced. In this sense, the instability arising from the bound (20) is not the tachyonic instability [3], but the GL instability. We stress that the tachyonic instability means negative mass squared $[-m_{\mp}^2$ in Eq.(16)] and thus, there is no unstable bound for (positive) mass parameter $(1/\lambda)$ like as (20).

4 Static scalar perturbation

In this section, we wish to develop the other criterion on checking the instability bound (20). This can be achieved by exploring the static scalar solutions to the linearized equation (9) on the background of Schwarzschild black hole. Considering the expression (13) with $\omega = 0$ ($\Omega = 0$), the radial equation of (9) for $u(r)$ can be rewritten as

$$\frac{r^5(r_+ - r)}{3r_+^2}u''(r) + \frac{r^4}{3r_+}u'(r) - \left[\frac{r^3}{3r_+} + \frac{l(l+1)r^4}{3r_+^2} \right]u(r) = \lambda^2 u(r). \quad (24)$$

Introducing a new coordinate $z = \frac{r}{r_+}$ [$z \in [1, \infty)$] and a new parameter $\lambda_s = \frac{\lambda}{r_+}$, Eq.(24) can be rewritten as

$$\frac{z^5(z-1)}{3}u''(z) + \frac{z^4}{3}u'(z) - \frac{z^4}{3} \left[\frac{1}{z} + l(l+1) \right]u(z) = \lambda_s^2 u(z), \quad (25)$$

which is independent of horizon radius r_+ . Here we focus on obtaining the $s(l=0)$ -mode solution. Because of the absence of analytic solution, one has to find a numerical solution. For this purpose, we firstly consider the near-horizon Taylor expansion for $u(z)$ as

$$u(z) = u_+ + u'_+(z-1) + \frac{u''_+}{2}(z-1)^2 + \dots, \quad (26)$$

which can be used to set data just outside the horizon for a numerical integration from the horizon to the infinity. Here we note that the coefficients u'_+ and u''_+ can be determined in terms of a free parameter u_+ as $u'_+ = (1 - 3\lambda_s^2)u_+$ and $u''_+ = \frac{3(3\lambda_s^2+2)}{2\lambda_s^6}u_+^2$.

On the other hand, an asymptotic form of $u(z)$ near $z = \infty$ is given by

$$u(z) = u_\infty + \frac{u^{(1)}}{z} + \frac{u^{(2)}}{z^2} + \dots. \quad (27)$$

Similarly, we find the relations of $u^{(1)} = u_\infty/2$ and $u^{(2)} = u_\infty/3$.

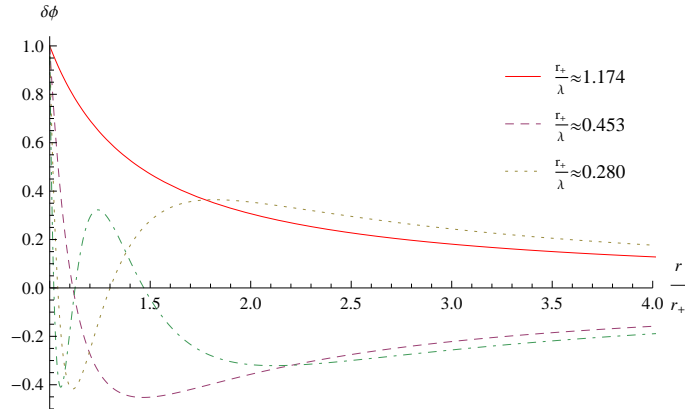


Figure 4: Graphs for scalar perturbation $\delta\phi$ as function of r/r_+ for $r_+/\lambda \approx 1.174, 0.453, 0.280$ which correspond to the number of nodes $n = 0, 1, 2$ in scalar profiles.

Now let us perform two integrations: from $z = 1$ to a matching point $z = z_m > 1$ by imposing the ingoing wave boundary condition at the horizon and from $z = \infty$ to $z = z_m$ by imposing no outgoing wave at infinity. Then, a numerical solution could be constructed by connecting the near-horizon form (26) to the asymptotic form (27) together with choosing a proper parameter λ_s . We obtain a discrete spectrum of parameter: $1/\lambda_s = r_+/\lambda \in [1.174, 0.453, 0.280, 0.202, \dots]$. In Fig. 4, these solutions are classified by order number $n = 0, 1, 2, 3, \dots$ which is identified with the number of nodes for $\delta\phi(z) = u(z)/z$. Here, a regular solution to equation (19) with $\Omega = 0$ is found only when the parameter λ takes a specific value $r_+/\lambda \approx 1.174$ (threshold of instability=the edge of domain of instability). In other words, the $n = 0$ scalar mode without zero represents a stable black hole, while the $n = 1, 2$ scalar modes with zero denote unstable black holes. This shows that one may classify the black hole into unstable and stable black holes by solving the static linearized scalar equation (25) without considering exponentially growing mode of $e^{\Omega t}$.

Finally, we note that the Schwarzschild solution without scalar hair ($\bar{\phi} = 0$) is allowed for any value of λ , while the black hole solution with scalar hair ($\bar{\phi} \neq 0$) exists when $\lambda/r_+(\lambda^2/M^2)$ belongs to a set of scalarization bands [3]. The key of instability is the appearance of zeros in the scalar profiles. Actually, the discrete set corresponds to the right-end values of scalarization bands for black hole with scalar hair. This shows a close connection between instability of black hole without scalar hair and appearance of black hole with scalar hair.

5 Discussions

First of all, we summarize similar properties for black holes in ESGB theory and Einstein-Weyl gravity in Table 1. This shows a strongly similar connection for Schwarzschild black hole between ESGB theory and Einstein-Weyl gravity even though two theories are different.

The s -mode of scalar perturbation around the Schwarzschild black hole induces the GL instability for the mass bound of $1/\lambda < 1.174/r_+$ in ESGB theory, while the s -mode of Ricci tensor perturbation around the Schwarzschild black hole induces the instability for the mass bound of $m < 0.876/r_+$ in Einstein-Weyl gravity. Also, the instability of Schwarzschild black hole without scalar hair implies the Gauss-Bonnet black hole with scalar hair in ESGB theory as the instability of Schwarzschild black hole without Ricci-tensor hair leads to the non-Schwarzschild black hole with Ricci hair in Einstein-Weyl gravity.

From this observation, we conclude that the instability of the Schwarzschild black hole in ESGB theory is interpreted as a scalar theory version of the GL instability for a small black hole in the tensor theory of Einstein-Weyl gravity. This instability dose not belong to the tachyonic instability because the scalar potential $V(r)$ is similar to $V_z(r)$ in (18) in Ref.[19], but it is quite different from $V_t(r)$ of the tachyon as was shown in Fig. 1.

Theory	ESGB theory	Einstein-Weyl gravity
Action	S_{ESGB} in (1)	S_{EW} in (10)
BH without hair	SBH with $\bar{\phi}(r) = \bar{R}_{\mu\nu} = 0$	SBH with $\bar{R}_{\mu\nu} = 0$
Linearized equation	scalar equation (9)	tensor equation (11)
GL instability mode	$s(l=0)$ -mode of $\delta\phi$	$s(l=0)$ -mode of $\delta R_{\mu\nu}$
Unstable mass bound	$0 < \frac{1}{\lambda} < \frac{1.174}{r_+}$	$0 < m < \frac{0.876}{r_+}$
Bifurcation point	1.174	0.876
Potential	$V(r)$ in (15)	$V_z(r)$ (18) in Ref.[19]
Small unstable SBH	$r_+ < r_c \approx 1.174$ for $\frac{1}{\lambda} = 1$	$r_+ < r_c \approx 0.876$ for $m = 1$
BH with hair	scalar hair in Refs.[2, 3]	Ricci-tensor hair in Ref.[13]

Table 1: Similar Properties for Schwarzschild black hole (SBH) in ESGB theory and Einstein-Weyl gravity.

Acknowledgments

This work was supported by the National Research Foundation of Korea (NRF) grant funded by the Korea government (MOE) (No. NRF-2017R1A2B4002057).

References

- [1] G. Antoniou, A. Bakopoulos and P. Kanti, Phys. Rev. Lett. **120**, no. 13, 131102 (2018) doi:10.1103/PhysRevLett.120.131102 [arXiv:1711.03390 [hep-th]].
- [2] D. D. Doneva and S. S. Yazadjiev, Phys. Rev. Lett. **120**, no. 13, 131103 (2018) doi:10.1103/PhysRevLett.120.131103 [arXiv:1711.01187 [gr-qc]].
- [3] H. O. Silva, J. Sakstein, L. Gualtieri, T. P. Sotiriou and E. Berti, Phys. Rev. Lett. **120**, no. 13, 131104 (2018) doi:10.1103/PhysRevLett.120.131104 [arXiv:1711.02080 [gr-qc]].
- [4] J. D. Bekenstein, Phys. Rev. D **51**, no. 12, R6608 (1995). doi:10.1103/PhysRevD.51.R6608
- [5] J. D. Bekenstein, Phys. Rev. Lett. **28**, 452 (1972). doi:10.1103/PhysRevLett.28.452
- [6] P. Bizon, Phys. Rev. Lett. **64**, 2844 (1990). doi:10.1103/PhysRevLett.64.2844
- [7] H. Luckock and I. Moss, Phys. Lett. B **176**, 341 (1986). doi:10.1016/0370-2693(86)90175-9
- [8] J. D. Bekenstein, Annals Phys. **82**, 535 (1974). doi:10.1016/0003-4916(74)90124-9
- [9] T. P. Sotiriou and V. Faraoni, Phys. Rev. Lett. **108**, 081103 (2012) doi:10.1103/PhysRevLett.108.081103 [arXiv:1109.6324 [gr-qc]].
- [10] L. Hui and A. Nicolis, Phys. Rev. Lett. **110**, 241104 (2013) doi:10.1103/PhysRevLett.110.241104 [arXiv:1202.1296 [hep-th]].
- [11] T. Regge and J. A. Wheeler, Phys. Rev. **108**, 1063 (1957). doi:10.1103/PhysRev.108.1063
- [12] F. J. Zerilli, Phys. Rev. Lett. **24**, 737 (1970). doi:10.1103/PhysRevLett.24.737
- [13] H. Lu, A. Perkins, C. N. Pope and K. S. Stelle, Phys. Rev. Lett. **114**, no. 17, 171601 (2015) doi:10.1103/PhysRevLett.114.171601 [arXiv:1502.01028 [hep-th]].
- [14] K. S. Stelle, Int. J. Mod. Phys. A **32**, no. 09, 1741012 (2017). doi:10.1142/S0217751X17410123

- [15] B. Whitt, *Phys. Rev. D* **32**, 379 (1985). doi:10.1103/PhysRevD.32.379
- [16] S. Mauro, R. Balbinot, A. Fabbri and I. L. Shapiro, *Eur. Phys. J. Plus* **130**, no. 7, 135 (2015) doi:10.1140/epjp/i2015-15135-0 [arXiv:1504.06756 [gr-qc]].
- [17] Y. S. Myung, *Phys. Rev. D* **88**, no. 2, 024039 (2013) doi:10.1103/PhysRevD.88.024039 [arXiv:1306.3725 [gr-qc]].
- [18] R. Gregory and R. Laflamme, *Phys. Rev. Lett.* **70**, 2837 (1993) doi:10.1103/PhysRevLett.70.2837 [hep-th/9301052].
- [19] H. L. A. Perkins, C. N. Pope and K. S. Stelle, *Phys. Rev. D* **96**, no. 4, 046006 (2017) doi:10.1103/PhysRevD.96.046006 [arXiv:1704.05493 [hep-th]].
- [20] G. Antoniou, A. Bakopoulos and P. Kanti, *Phys. Rev. D* **97**, no. 8, 084037 (2018) doi:10.1103/PhysRevD.97.084037 [arXiv:1711.07431 [hep-th]].
- [21] G. N. Felder, L. Kofman and A. D. Linde, *Phys. Rev. D* **64**, 123517 (2001) doi:10.1103/PhysRevD.64.123517 [hep-th/0106179].
- [22] H. Kodama and A. Ishibashi, *Prog. Theor. Phys.* **111**, 29 (2004) doi:10.1143/PTP.111.29 [hep-th/0308128].
- [23] T. Moon and Y. S. Myung, *Phys. Rev. D* **88**, no. 12, 124014 (2013) doi:10.1103/PhysRevD.88.124014 [arXiv:1310.3024 [hep-th]].